SHP-2 Tyrosine Phosphatase as an Intracellular Target of *Helicobacter pylori* CagA Protein

Hideaki Higashi,[1] Ryouhei Tsutsumi,[1] Syuichi Muto,[1] Toshiro Sugiyama,[2] Takeshi Azuma,[3] Masahiro Asaka,[2] Masanori Hatakeyama[1]*

Helicobacter pylori CagA protein is associated with severe gastritis and gastric carcinoma. CagA is injected from the attached *Helicobacter pylori* into host cells and undergoes tyrosine phosphorylation. Wild-type but not phosphorylation-resistant CagA induced a growth factor–like response in gastric epithelial cells. Furthermore, CagA formed a physical complex with the SRC homology 2 domain (SH2)–containing tyrosine phosphatase SHP-2 in a phosphorylation-dependent manner and stimulated the phosphatase activity. Disruption of the CagA–SHP-2 complex abolished the CagA-dependent cellular response. Conversely, the CagA effect on cells was reproduced by constitutively active SHP-2. Thus, upon translocation, CagA perturbs cellular functions by deregulating SHP-2.

Helicobacter pylori, which infects about 50% of the world's population, causes gastric diseases ranging from gastritis to cancer and has been classified as a group I carcinogen. CagA is the product of the *cagA* gene, which is carried in virulent type I strains of *H. pylori*. The correlation between expression of CagA and *H. pylori* virulence has been well-documented (*1*–*4*). In particular, increased frequency of gastric carcinoma and MALT (mucosal-associated lymphoid tissue) lymphoma in patients infected with *cagA*$^+$ *H. pylori* strains suggests that CagA is associated with an increased risk of gastric cancer. However, no direct role for CagA in pathogenesis or function has been described.

After attachment of *cagA*$^+$ *H. pylori* to gastric epithelial cells, CagA is directly injected from the bacteria into the cells via the bacterial type IV secretion system and undergoes tyrosine phosphorylation in the host cells (*5*–*9*). The *cagA*$^+$ *H. pylori*–host cell interaction also triggers morphological changes similar to those induced by growth factor (*5*). Translocated CagA may be involved in dysregulation of host cell functions, thereby contributing to pathogenesis.

To examine the role of the CagA protein in the host cell, the *cagA* gene isolated from the *H. pylori* standard strain NCTC11637 was COOH-terminal–tagged with the hemagglutinin (HA) and was cloned into pSP65SRα. The expression vector was transfected into AGS human gastric epithelial cells or monkey COS-7 cells, and CagA expression was confirmed by immunoblotting with antibody to HA (Fig. 1A) (*10*, *11*). Immunoblotting with antibody to phosphotyrosine revealed that the expressed CagA underwent tyrosine phosphorylation (Fig. 1A). The NCTC11637-derived CagA protein possesses seven potential tyrosine phosphorylation sites (residues -117, -893, -912, -965, -999, -1033, and -1100). Of these, residues -893, -912, -965, -999, and -1033 constitute five copies of the EPIYA sequences. Notably, residues -965, -999, and -1033 are made by three repeats of the "D1+D2+D3" element (*12*). We generated a CagA mutant in which all of the tyrosine residues present in the five copies of the Glu-Pro-Ile-Tyr-Ala (EPIYA) sequences were replaced by alanine. The mutant CagA did not undergo any tyrosine phosphorylation in cells (Fig. 1A). Thus, one or several of these tyrosine residues were apparently in vivo tyrosine phosphorylation sites of CagA.

AGS cells contacted with *cagA*$^+$ *H. pylori* respond by producing the hummingbird phenotype, characterized by elongation and spreading of cells (*5*). We examined morphological changes in AGS cells after transfection of the CagA expression vector. At 17 hours after transfection, 20 to 30% of the cells (transfection efficiency was approximately 40%) exhibited the hummingbird phenotype (Fig. 1B). In contrast, phosphorylation-resistant CagA failed to induce any morphological changes in AGS cells. Thus, CagA was the necessary and sufficient *H. pylori* component for the hummingbird phenotype, and tyrosine phosphorylation of CagA was required. CagA preferentially local-

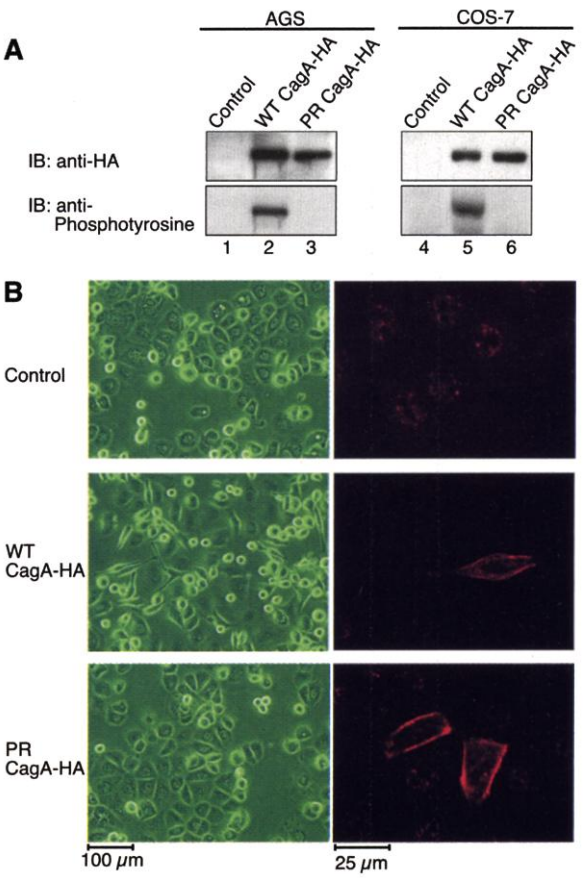

Fig. 1. Ectopic expression of CagA. (**A**) AGS or COS-7 cells were transiently transfected with HA-tagged wild-type (WT) CagA, HA-tagged phosphorylation-resistant (PR) CagA or an empty vector (control). Cell lysates were immunoblotted (IB) with antibody to HA or phosphotyrosine. (**B**) The morphology of AGS cells transfected with CagA was examined under a microscope at 17 hours after transfection (left). The cells were stained with an antibody to HA (right).

[1]Division of Molecular Oncology, Institute for Genetic Medicine and Graduate School of Science, Hokkaido University, Sapporo 060-0815, Japan. [2]Department of Gastroenterology & Hematology, Graduate School of Medicine, Hokkaido University, Sapporo 060-0815, Japan. [3]The Second Department of Internal Medicine, Fukui Medical University, Fukui 910-1193, Japan.

*To whom correspondence should be addressed. E-mail: mhata@imm.hokudai.ac.jp

izes in the plasma membrane (*13*), but this membrane localization was independent of tyrosine phosphorylation and was also observed in the case of phosphorylation-resistant CagA (Fig. 1B).

The hummingbird phenotype resembles the morphological changes caused by exposure to hepatocyte growth factor (HGF) (*5*). Other reports suggest that activation of SHP-2 (*14–16*), a cytoplasmic tyrosine phosphatase that contains two tandem SH2 domains, plays a major role in the HGF-induced cellular morphological changes (*17*). Indeed, SHP-2 positively regulates signal transduction events from a variety of activated receptor tyrosine kinases (*14–16*). We found that SHP-2 was expressed in AGS cells, whereas SHP-1, another SH2-containing phosphatase, was hardly detectable (*18*). Because SH2 domains are phosphotyrosine-binding modules (*19*), we investigated the capacity of CagA to bind SHP-2. In lysates from AGS cells transfected with the CagA expression vector, CagA co-immunoprecipitated endogenous SHP-2 and vice versa (Fig. 2A). In contrast, the phosphorylation-resistant CagA and SHP-2 did not co-immunoprecipitate each other. Furthermore, SHP-2 failed to co-immunoprecipitate unphosphorylated CagA (Fig. 2A). Thus, CagA binds SHP-2 in gastric epithelial cells in a tyrosine phosphorylation-dependent manner. Furthermore, immunodepletion of SHP-2 from the lysates of AGS cells expressing CagA simultaneously depleted almost all, if not all, of the tyrosine-phosphorylated CagA from the lysates (Fig. 2B). Thus, tyrosine-phosphorylated CagA binds SHP-2 stoichiometrically in these cells.

Physical interaction between tyrosine-phosphorylated CagA and SHP-2 was also demonstrated in COS-7 cells (Fig. 3A). Using the COS-7 cells, we examined regions in SHP-2 that are required for CagA binding. A SHP-2 mutant lacking the SH2 domains (SHP-2ΔSH2-Myc) had totally lost the ability to bind CagA, whereas another mutant lacking the phosphatase domain (SHP-2ΔPD-Myc) retained CagA-binding activity (Fig. 3B) (*20*). Thus, tyrosine-phosphorylated CagA appears to interact specifically with the SH2 domains of SHP-2.

Binding of phosphotyrosine-peptide to the SH2 domains of SHP-2 is considered to relieve the autoinhibitory mechanism and reveal its previously latent phosphatase activity (*21–25*). To determine whether this is also the case with the CagA-SHP-2 interaction, we expressed the Myc-tagged SHP-2 in the presence or absence of CagA in COS-7 cells and we immunoprecipitated SHP-2 with an antibody to Myc. The immune complex was then subjected to an in vitro phosphatase assay (*26*). Phosphatase activity of SHP-2 was potently stimulated when it formed a complex with CagA (Fig. 3C).

We next investigated whether the CagA-SHP-2 complex was involved in the induction of the hummingbird phenotype. Expression of CagA together with the phosphatase-defective SHP-2ΔPD-Myc, which still interacts physically with CagA via the SH2 domains (Fig. 3B), strongly reduced the induction of the hummingbird phenotype (Fig. 4A). To rule out the possibility that SHP-2ΔPD-Myc competitively inhibited the binding of CagA with SH2-containing molecules other than SHP-2 that are involved in the hummingbird phenotype, we ectopically expressed wild-type SHP-2, which, like SHP-2ΔPD-Myc, should act as a competitor for such molecules if they exist. Despite twofold higher levels than those of SHP-2ΔPD-Myc, wild-type SHP-2 did not inhibit the hummingbird phenotype by CagA (Fig. 4A), arguing against the existence of such molecules. Thus, complex formation of CagA and endogenous SHP-2 is an essential prerequisite for the induction of the hummingbird phenotype in AGS cells. Moreover, treatment of CagA-expressing AGS cells with an SHP-2-specific phosphatase inhibitor, calpeptin (*27*), inhibited the induction of the hummingbird phenotype (Fig. 4B), indicating that SHP-2 phosphatase activity is required for the morphological changes.

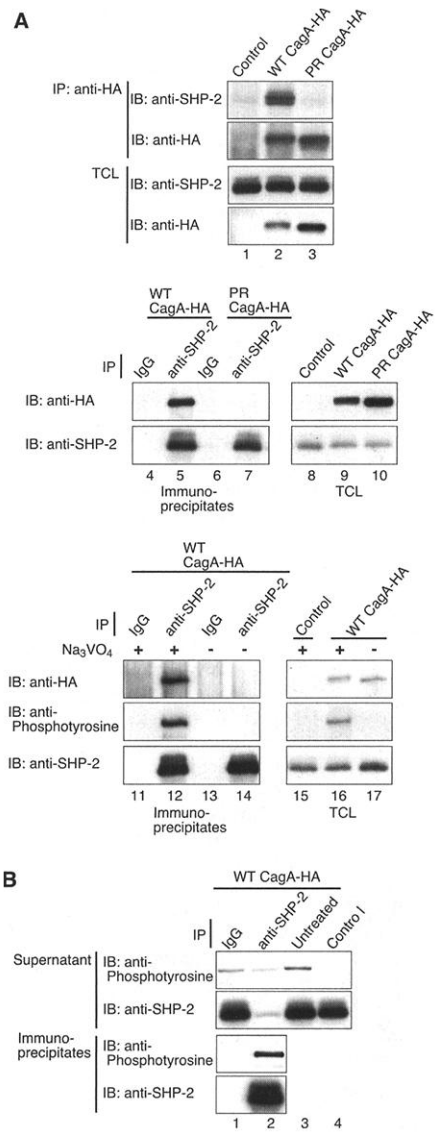

Fig. 2. Interaction between CagA and SHP-2. **(A)** AGS cells were transfected with WT CagA-HA, PR CagA-HA, or a control empty vector. WT CagA-HA or SHP-2 was immunoprecipitated from lysates prepared in the presence or absence of Na_3VO_4, a tyrosine phosphatase inhibitor. The immunoprecipitates (IP) and total cell lysates (TCL) were immunoblotted (IB) with antibodies as described. Pre-immune rabbit IgG was used for a control antibody. **(B)** Amounts of tyrosine-phosphorylated CagA in the supernatants of AGS cells transfected with WT CagA-HA before and after immunodepletion with antibody to SHP-2 or the control antibody.

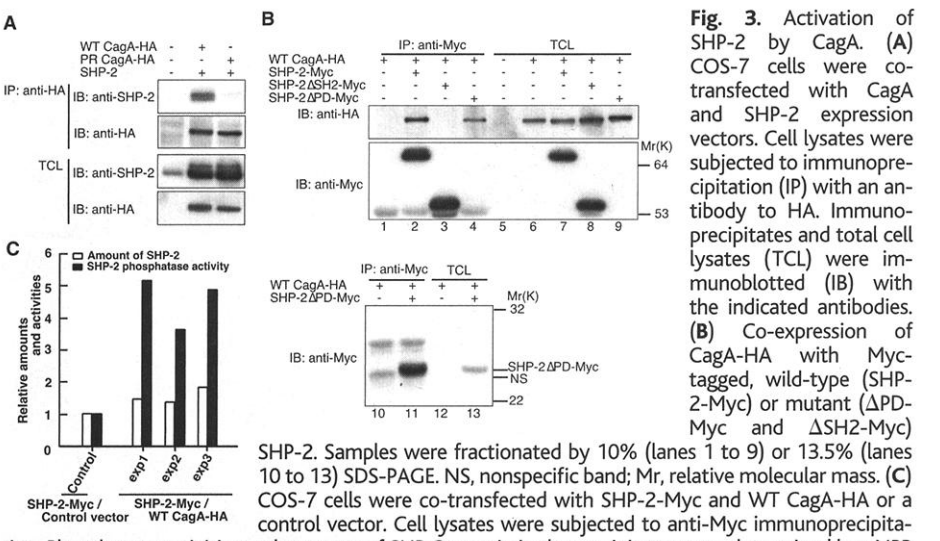

Fig. 3. Activation of SHP-2 by CagA. **(A)** COS-7 cells were co-transfected with CagA and SHP-2 expression vectors. Cell lysates were subjected to immunoprecipitation (IP) with an antibody to HA. Immunoprecipitates and total cell lysates (TCL) were immunoblotted (IB) with the indicated antibodies. **(B)** Co-expression of CagA-HA with Myc-tagged, wild-type (SHP-2-Myc) or mutant (ΔPD-Myc and ΔSH2-Myc) SHP-2. Samples were fractionated by 10% (lanes 1 to 9) or 13.5% (lanes 10 to 13) SDS-PAGE. NS, nonspecific band; Mr, relative molecular mass. **(C)** COS-7 cells were co-transfected with SHP-2-Myc and WT CagA-HA or a control vector. Cell lysates were subjected to anti-Myc immunoprecipitation. Phosphatase activities and amounts of SHP-2 protein in the precipitates were determined by *p*NPP assay and anti-SHP-2 immunoblotting, respectively. Intensities of chemiluminescence on the immunoblotted filter were quantitated using a luminescent image analyzer LAS1000 (FUJIFILM, Tokyo, Japan). The relative amount and phosphatase activity were calculated with the value for SHP-2 immunoprecipitates in the absence of CagA taken as a control.

Lastly, we investigated whether SHP-2 was capable of inducing the hummingbird-like morphological changes in the absence of CagA. Because CagA is cell membrane–associated (Fig. 1B), recruitment of SHP-2 by CagA may serve as a mechanism for relocalization of the cytoplasmic phosphatase to the cell membrane. Accordingly, we generated a membrane-targeted, constitutively active SHP-2 by adding the membrane-localization signal derived from v-Src (*28*) to the SHP-2 mutant lacking the SH2 domains (Myr-SHP-2ΔSH2-Myc) (*20*, *23*, *24*). Ectopic expression of Myr-SHP-2ΔSH2-Myc in AGS cells provoked cellular morphological changes indistinguishable from the hummingbird phenotype induced by CagA (Fig. 4, C and D) (*13*). On the other hand, constitutively active SHP-2 lacking the membrane-targeting signal (SHP-2ΔSH2-Myc) was incapable of inducing the morphological changes (Fig. 4C). Thus, membrane-tethering of activated SHP-2 was necessary and sufficient for the induction of the hummingbird phenotype.

We demonstrate here that *H. pylori* virulence factor CagA, which is translocated from the bacteria into gastric epithelial cells (*5*–*9*), can perturb mammalian signal transduction machineries and modify cellular functions by physically interacting with a host cell protein, SHP-2. SHP-2, like its *Drosophila* homolog Corkscrew, is known to play an important positive role in the mitogenic signal transduction that connects receptor tyrosine kinases and ras (*14*, *15*). Also, SHP-2 is actively involved in the regulation of spreading, migration, and adhesion of cells (*29*–*32*). Deregulation of SHP-2 by CagA may induce abnormal proliferation and movement of gastric epithelial cells, promoting the acquisition of a cellular transformed phenotype. Our results provide a molecular basis for the pathological actions of CagA on gastric epithelial cells.

CagA is noted for its amino acid sequence diversity among different *H. pylori* strains. The phosphorylation of the EPIYA motif is located in the repeat region of CagA and is expanded by duplication. Accordingly, the number and sequence polymorphism of the CagA phosphorylation sites, which collectively determine binding affinity of CagA to SHP-2, may be important variables in determining the clinical outcome of infection by different *cagA*$^+$ *H. pylori* strains.

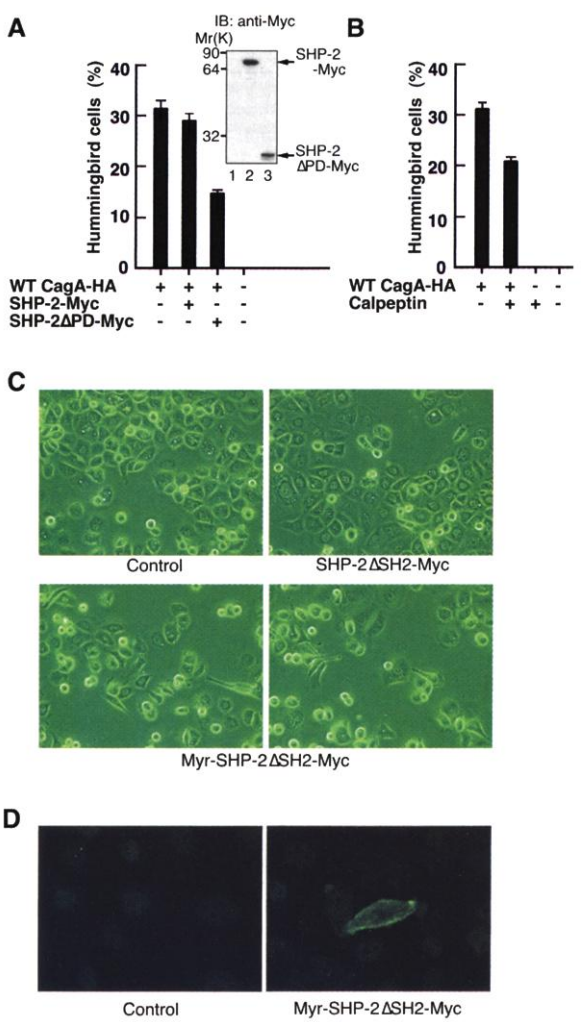

Fig. 4. Role of SHP-2 in inducing hummingbird phenotype. (**A**) AGS cells were transiently co-transfected with WT CagA-HA and SHP-2-Myc or SHP-2ΔPD-Myc (n=3). Induction of the hummingbird phenotype and expressions of SHP-2-Myc and SHP2ΔPD-Myc proteins in the transfected AGS cells. Cells showing the hummingbird phenotype were counted in 10 different fields in each of three dishes (the area of one field being 0.25 mm^2). (**B**) Cells transfected with CagA-HA were treated with either 100 μg/ml calpeptin or a vehicle for 1 hour before analysis (n=3). (**C**) Morphology of AGS cells transfected with SHP-2ΔSH2-Myc with or without the membrane-targeting sequence (Myr-) at 15 hours after transfection. (**D**) Cells expressing Myr-SHP-2ΔSH2-Myc were stained with an anti-Myc antibody.

References and Notes

1. A. Covacci, J. L. Telford, G. D. Giudice, J. Parsonnet, R. Rappuoli, *Science* **284**, 1328 (1999).
2. M. J. Blaser *et al.*, *Cancer Res.* **55**, 2111 (1995).
3. E. J. Kuipers, G. I. Perez-Perez, S. G. Meuwissen, M. J. Blaser, *J. Natl. Cancer Inst.* **87**, 1777 (1995).
4. J. Personnet, G. D. Friedman, N. Orentreich, H. Vogelman, *Gut* **40**, 297 (1997).
5. E. D. Segal, J. Cha, J. Lo, S. Falkow, L. S. Tompkins, *Proc. Natl. Açad. Sci. U.S.A.* **96**, 14559 (1999).
6. M. Asahi *et al.*, *J. Exp. Med.* **191**, 593 (2000).
7. M. Stein, R. Rappuoli, A. Covacci, *Proc. Natl. Acad. Sci. U.S.A.* **97**, 1263 (2000).
8. S. Odenbreit *et al.*, *Science* **287**, 1497 (2000).
9. S. Backert *et al.*, *Cell. Microbiol.* **2**, 155 (2000).
10. Thirty μg of plasmids were transfected into AGS cells (1.8 x 10^6 cells) using Lipofectamine 2000 reagent (Invitrogen, Carlsbad, CA). COS-7 cells (1.5 × 10^6 cells) were transfected with 20 μg of plasmids using the calcium phosphate method. Cells were harvested at 36 hours after transfection and lysed in lysis buffer (Tris-HCl at pH 7.5, 100 mM NaCl, 5 mM EDTA, and 1% Brij-35) containing 2 mM of Na_3VO_4, 2 mM of phenylmethylsulfonyl fluoride (PMSF), 10 μg/ml of leupeptin, 10 μg/ml of trypsin inhibitor, and 10 μg/ml of aprotinin. The lysates were treated with appropriate antibodies and the immune complexes were trapped on protein A– or G Sepharose beads. The immunoprecipitates were subjected to SDS-polyacrylamide gel (SDS-PAGE).
11. Antibodies used were anti-HA antibodies Y-11 (Santa Cruz, Santa Cruz, CA) and 12CA5, antibody to Myc (antibody 9E10), antibody to SHP-2 (antibody C-18) (Santa Cruz), and antibody to phosphotyrosine (antibody 4G10) (Upstate Biotechnology, Lake Placid, NY).
12. A. Covacci *et al.*, *Proc. Natl. Acad. Sci. U.S.A.* **90**, 5791 (1993).
13. AGS cells transfected with CagA-HA or SHP-2-Myc were fixed with 3% paraformaldehyde. Cells were then treated with antibody to HA (Y-11) or antibody to Myc (9E10). Primary antibodies were localized by Alexa Fluor 546-conjugated anti-rabbit or Alexa Fluor 488-conjugated anti-mouse antibody (Molecular Probes, Eugene, OR). Images were acquired using a confocal microscope system (Fluoview, Olympus, Tokyo, Japan).
14. G. S. Feng, C. C. Hui, T. Pawson, *Science* **259**, 1607 (1993).
15. R. M. Jr. Freeman, J. Plutzky, B. G. Neel, *Proc. Natl. Acad. Sci. U.S.A.* **89**, 11239 (1992).
16. S. Ahmad, D. Banville, Z. Zhao, E. H. Fischer, S. H. Shen, *Proc. Natl. Acad. Sci. U.S.A.* **90**, 2197 (1993).
17. A. Kodama *et al.*, *Mol. Biol. Cell* **11**, 2565 (2000).
18. H. Higashi *et al.*, unpublished data.
19. Z. Songyang *et al.*, *Cell* **72**, 767 (1993).
20. SHP-2ΔPD-Myc consists of amino acid residues 1 to 192 of SHP-2-Myc. SHP-2ΔSH2-Myc lacks amino acid sequences between 33 and 191 of SHP-2-Myc. Myr-SHP-2ΔSH2-Myc was made by replacing the NH_2-terminal 32 amino acids of SHP-2ΔSH2-Myc with the myristoylation signal sequence of v-Src (*28*). The DNAs were inserted into pSP65SRα vector.
21. R. J. Lechleider *et al.*, *J. Biol. Chem.* **268**, 21478 (1993).
22. S. Pluskey, T. J. Wandless, C. T. Walsh, S. E. Shoelson, *J. Biol. Chem.* **270**, 2897 (1995).
23. Z. Zhao, R. Larocque, W. T. Ho, E. H. Fischer, S. H. Shen, *J. Biol. Chem.* **269**, 8780 (1994).
24. U. Dechert, M. Adam, K. W. Harder, I. Clark-Lewis, F. Jirik, *J. Biol. Chem.* **269**, 5602 (1994).
25. P. Hof, S. Pluskey, S. Dhe-Paganon, M. J. Ech, S. E. Shoelson, *Cell* **92**, 441 (1998).
26. SHP-2 phosphatase activity was measured with the use of *p*-nitrophenyl phosphate (*p*NPP) as a substrate. SHP-2 immunoprecipitates were incubated in phosphatase assay buffer (100 mM sodium acetate at pH 5.0 and 1.6 mM dithiothreitol) containing 10 mM

pNPP at 30°C for 1 hour. Absorbance of the reaction mixture was measured at 410 nm.
27. S. M. Schoenwaelder *et al.*, *Curr. Biol.* **10**, 1523 (2000).
28. D. M. Spencer, T. J. Wandless, S. L. Schreiber, G. R. Crabtree, *Science* **262**, 1019 (1993).
29. T. M. Saxton *et al.*, *EMBO J.* **16**, 2352 (1997).
30. S. Manes *et al.*, *Mol. Cell. Biol.* **19**, 3125 (1999).
31. E. S. Oh *et al.*, *Mol. Cell. Biol.* **19**, 3205 (1999).
32. D. H. Yu, C. K. Qu, O. Henegariu, X. Lu, G. S. Feng, *J. Biol. Chem.* **273**, 21125 (1998).
33. We thank R. A. Weinberg for reading of the manuscript. We also thank T. Matozaki for human SHP-2 cDNA. Supported by a Grant-in Aid for Scientific Research on Priority Areas from the Ministry of Education, Culture, Sports, Science and Technology of Japan; a Research Grant from the Human Frontier Science Program Organization; and a Research Grant from the Nippon Boehringer Ingelheim Co., Ltd.

16 October 2001; accepted 4 December 2001
Published online 13 December 2001;
10.1126/science.1067147
Include this information when citing this paper.

Immunoglobulin-Domain Proteins Required for Maintenance of Ventral Nerve Cord Organization

Oscar Aurelio,[1] David H. Hall,[2] Oliver Hobert[1]*

During development, neurons extend axons along defined routes to specific target cells. We show that additional mechanisms ensure that axons maintain their correct positioning in defined axonal tracts. After termination of axonal outgrowth and target recognition, axons in the ventral nerve cord (VNC) of *Caenorhabditis elegans* require the presence of a specific VNC neuron, PVT, to maintain their correct positioning in the left and right fascicles of the VNC. PVT may exert its stabilizing function by the temporally tightly controlled secretion of 2-immunoglobulin (Ig)–domain proteins encoded by the *zig* genes. Dedicated axon maintenance mechanisms may be widely used to ensure the preservation of functional neuronal circuitries.

The development of axonal tracts in the nervous system depends on defined and tightly regulated interactions between individual cell types that ultimately guide axons to their specific targets. In the nematode *C. elegans*, the PVT interneuron plays a prominent role during the development of the ventral nerve cord (VNC). The cell body of PVT is located at the posterior end of the VNC and its axon, which is one of the first to pioneer the VNC (*1*), extends along the entire length of the right VNC from the posterior of the animal into the anteriorly located nerve ring (*2*). PVT transiently expresses the *unc-6*/netrin guidance cue during embryonic development (*3*) and embryonic ablation of PVT as well as mutations in *unc-6*/netrin cause defects in dorso-ventral axon attraction into the VNC (*4*).

Various aspects of axon pathfinding and target recognition are regulated by members of the immunoglobulin superfamily (IgSF) of secreted and cell surface bound proteins (*5*). In a comprehensive and genome-wide analysis of expression patterns of IgSF proteins in *C. elegans* (*6*), we noted that six members of a novel family of secreted 2-Ig domain proteins, termed *zig-1*, *zig-2*, *zig-3*, *zig-4*, *zig-5*, and *zig-8* (Fig. 1A), are co-expressed in the PVT neuron of larval and adult stage animals (Fig. 1, B and C). Given the previously established embryonic role of PVT in axon guidance in mid-embryonic stages, we were intrigued to find that the onset of expression of all six PVT-expressed *zig* reporter gene constructs occurred significantly later than the stages of embryonic VNC axon outgrowth; this is particularly apparent with *zig-1::gfp*, *zig-2::gfp*, *zig-3::gfp*, *zig-4::gfp*, and *zig-8::gfp*, whose expression is activated postembryonically in the first larval (L1) stage (Fig. 1, D and E). This expression profile prompted us to investigate a potential postembryonic role of PVT by assessing the effect of its microsurgical removal in the L1 stage. Using a reporter gene that labels the complete VNC, we noted that 30% of animals in which PVT was laser ablated in the L1 stage contained axons that were aberrantly placed across the ventral midline (Fig. 2, B through D). By ablating PVT in the L1 stage of animals in which various subsets of neurons in the VNC are labeled with *gfp* (*7*), we determined that the misplaced axons derived from the AVKL/R, PVQL/R, HSNL/R, and RMEV neuron classes (Fig. 2, A, C, and D). With the exception of HSNL/R, the axons of all these neuron classes have completed their outgrowth in mid- to late embryonic stages, i.e., long before we ablated PVT in the first larval stage. The observation that PVT ablation in the L1 stage disrupts the correct positioning of embryonically generated axons thus reveals an unexpected nonautonomous role for a neuron in maintaining VNC architecture past the stage of its initial patterning.

PVT is required to exert its maintenance function during a narrowly defined temporal window. Laser ablation of PVT at the L1, L2, and adult stages revealed that PVT function is only required during the L1 stage (Fig. 2D). Moreover, individual PVT-ablated animals that were scored at any stage later than the L1 stage as either "wild type" or "defective," still showed the same phenotype when scored 2 days after the initial scoring (n = 14). Thus, axons that have drifted in the L1 stage, will remain in the inappropriate track, while axons that managed to remain in the correct position, will not flip over at later stages. One explanation for the stability of the phenotype past the L1 stage could be the growth of the physical barrier presented by the hypodermal ridge, which significantly increases its size during larval development (*8*). Another, not mutually exclusive possibility for the stability of the phenotype is that a drifted axon is kept in the opposite cord by homophilic interaction with the axon of its contralateral analog (*9*). Double laser ablations revealed this to be indeed the case. In the absence of PVT, the aberrant axon flip-over of PVQL into the right VNC is suppressed if PVQR is ablated (Fig. 2D).

We also considered the possibility that axon flip-over into the opposite fascicle in PVT-ablated animals may be facilitated by the mechanical force provided by the constant bending of animals along their longitudinal axis during sinusoidal locomotion of the animals. We tested this hypothesis by culturing PVT-ablated L1 animals on plates that contain the cholinergic agonist levamisole, which immobilizes animals due to hypercontraction of their body wall muscles (*10*). In an independent approach, we ablated PVT in muscle-defective *unc-97* animals (*11*). Both immobilization protocols caused a complete suppression of the axon flip-over phenotype upon PVT ablation (Fig. 2D), suggesting that movement and hence mechanical force is a contributing factor for the axon flip-over.

Taken together, our data suggest that specifically at the L1 stage the left and right VNC are intrinsically unstable structures that require the presence of a specific neuron to maintain the integrity of individual axonal tracts (Fig. 2E). PVT presumably supplies stabilizing cues that prevent axons from drifting into the opposite fascicle, an event that is facilitated by mechanical force and homophilic attraction of bilaterally analogous axons in the opposite fascicle. Stabilizing cues provided by PVT either directly help to anchor axons in the left or right

[1]Department of Biochemistry and Molecular Biophysics, Center for Neurobiology and Behavior, Columbia University, College of Physicians and Surgeons, New York, NY 10032, USA. [2]Center for *C. elegans* Anatomy, Albert Einstein College of Medicine, Department of Neuroscience, Bronx, NY 10461, USA.

*To whom correspondence should be addressed. E-mail: or38@columbia.edu